

Development of a Laser Ablation Isochron K-Ar Dating Instrument for Landing Planetary Missions. Y. Cho¹, Y. N. Miura² and S. Sugita^{1,3}, ¹Dept. of Earth and Planetary Science, Univ. Tokyo (5-1-5 Kashiwanoha, Kashiwa, Chiba, Japan; cho@astrobio.k.u-tokyo.ac.jp), ²Earthquake Research Institute, Univ. Tokyo (1-1-1 Yayoi, Bunkyo-ku, Tokyo, Japan), ³Dept. Complexity Science and Engineering, Univ. Tokyo (5-1-5 Kashiwanoha, Kashiwa, Chiba, Japan).

Introduction: The crater chronology function estimated for Mars has uncertainty as large as 1 Gyr [1]. This is because no Martian sample has been obtained with information which geologic unit it is from. In order to accurately constrain Martian history, such as the transition in climate phase and volcanic history, acquiring absolute chronology is essential. It is rather obvious that sample return missions from Mars or the Moon will provide accurate and precise age data and yield best results to calibrate crater chronology function on the planets. Because a round-trip between the Earth and Mars is technologically challenging and requires large budget, however, opportunities for explorations are very limited and extremely precious. Thus, samples to be returned to the Earth need be good to representatives for the geologic unit around the landing point. Because in-situ dating allows for iterative measurements on the planetary surfaces to find the best samples to bring back, sample return missions and in-situ dating are complementary to each other.

We have been developing an in-situ dating method using K-Ar system for planetary landing missions [2,3]. The K-Ar dating method employs radiometric decay of ⁴⁰K into ⁴⁰Ar with half-life of 1.27 Gyr [4]. The K-Ar dating method is relatively viable compared to other dating methods, such as Ar-Ar, U-Pb, and Sr-Rb dating, because K is relatively abundant in the igneous rocks and Ar can be easily extracted (i.e., simply heat the sample), which leads to a simpler instrumental configuration.

In this paper, we report our first age determination results using our bread board model.

Measurement system: Our system measures K and Ar with two techniques at the same laser irradiation spot on a sample: laser-induced breakdown spectroscopy (LIBS) and quadrupole mass spectrometry (QMS), respectively (LIBS-QMS system). K and Ar are extracted from a sample simultaneously by the laser ablation, in which the sample is vaporized by a series of intense laser pulses. Spot-by-spot analyses using the laser ablation technique enable the isochron measurement from a single rock sample, providing higher reliability compared with the whole rock analysis as proposed previously [e.g., 5, 6].

Figure 1 shows the schematic diagram of the instrument. A rock sample is set in the vacuum chamber. The chamber is evacuated and kept at $\sim 10^{-6}$ Pa by a

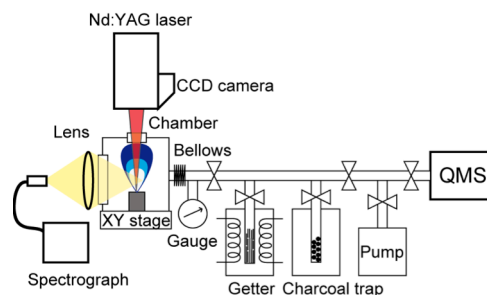


Fig. 1: Schematic diagram of the LIBS-QMS system.

turbo-molecular pump, in order to maintain background Ar level low. The system is equipped with a Ti-Zr getter and a charcoal cold trap. The getter is heated at 700-800 °C to purify the gas extracted from the sample. The charcoal trap adsorbs heavy noble gases (Ar through Xe) when cooled at the temperature of liquid nitrogen.

We used a Nd:YAG laser with 6 ns of pulse width and 1064 nm of wavelength (Surelite I, Continuum). The laser energy was set at 100 mJ and the spot diameter was ~ 500 μ m. We used a small spectrometer (HR 2000+, Ocean Photonics Inc.) with a charge couple device (CCD), to simulate a small and simple spectro for the spacecraft missions. The light emission from plasma was collected by a lens and transmitted through an optical fiber to the entrance slit of the spectrograph. The spectral acquisition time was 1 ms and the spectrograph shutter was opened before the laser pulses reached the sample; time-integrated plasma emission was observed to simulate a non-gated operations on the planetary missions.

A quadrupole mass spectrometer (M-201QA-TDM, Canon-Anelva) is used to measure the Ar isotopes such as ⁴⁰Ar and ³⁶Ar.

A couple of practical problems are described in the followings. In order to enhance the sensitivity of Ar detection, the volume of the chamber must be minimized. Then the rock vapor generated by laser ablation adheres the viewport for LIBS measurements, prohibiting the accurate LIBS measurement when the viewport is placed directly above the sample. Another technical challenge associated with reduction in emission line intensity under vacuum conditions ($p < \sim 10^{-2}$ Pa); emission intensity decreases by an order of magnitude compared with that in atmospheric pressure [7]. We

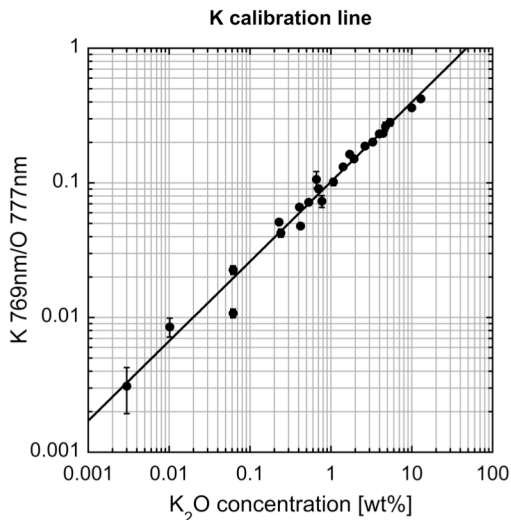


Fig. 2: Calibration line of K_2O concentration.

have resolve these problems at least partially by placing the window on the side of the chamber where the ejected plasma vapor does not reach. Another advantage of this alignment is that the light collection lens can be placed very close to the plasma, leading to a larger solid angle for light collection for the weak K emission under vacuum conditions.

Calibration of K and Ar measurement:

LIBS calibration. In order to construct a calibration curve for K_2O for our system, 24 geologic samples with known K_2O concentration (between 30 ppm and 12 wt%) were measured with the LIBS technique. The calibration samples were pellets made of rock powders certified by USGS and AIST (Japan Geological Survey). Figure 2 shows the calibration line for K_2O for our system. One hundred laser shots were recorded separately and averaged to enhance the signal-to-noise ratio. Background spectra are also averaged over 100 times and subtracted from each spectrum. The intensity of the emission lines were calculated from the peak areas acquired with peak-fitting analyses with Gaussian. We measured four spots per a sample to estimate standard deviation (shown by the error bars in Fig. 2).

Although the strongest line of K is at 766.4 nm, a probable Mg emission line also occurs at 766.4 nm, which makes line separation between these two elements impossible in our current resolution. Thus, we used the second strongest emission line at 769.9 nm for our calibration. The intensity of K line was normalized by that of the O emission line at 777 nm, reducing the effects of the fluctuation in signal strength due to several experimental conditions, such as laser energy and the surface condition of the sample.

The calibration line is not linear and exhibits a roll over at the high K_2O concentrations. This is the most

likely due to the self-absorption effect, which is not observed by Stipe et al. [8]. This apparent difference is probably due to whether high-speed gating is used; Stipe et al. [8] uses high-speed gating with an intensified CCD. The calibration line was fitted by a power law: $I=0.10C^{0.59}$, where I and C are the intensity of K 769 nm line divided by that of O 777 nm line, and K_2O concentration, respectively. Note that the accuracy deteriorates at $K_2O>5$ wt%, where the single power law does not follow the experimental data.

Errors in the calibration were estimated as:

$$\frac{([K_2O]_{\text{measured}}-[K_2O]_{\text{certified}})/[K_2O]_{\text{certified}} \times 100 [\%]}{}$$

The percent accuracy for the LIBS calibration was estimated to be ~15% and ~10% for $[K_2O]=1$ and 7 wt%, respectively. We used these values to estimate the calibration errors for the age measurements below.

The detection limit for K_2O was calculated by $LOD=3s_{bi}m$, where s_{bi} and m are the standard deviation of the blank measures and the slope of the calibration curve, respectively. When we substitute $s_{bi}=1 \times 10^{-3}$ for a sample which does not contain K_2O and $m=0.12$ (the result of linear fitting with $K_2O < 0.24$ wt% data), 3.6 ppm of LOD is obtained. The limit of quantification, given by $LOQ=10s_{bi}m$, was 12 ppm. The detection limit is controlled by the competition between K emission intensity and the dark noise level of the CCD.

QMS calibration. The correlation between ion current [A] of QMS and the amount [cm^3 STP] (STP: standard temperature and pressure) of released Ar gas was calibrated by introducing the known amount of atmospheric ^{40}Ar to the system. To determine the absolute amount of ^{40}Ar , we have made an auxiliary vacuum line, which consists of a pipette with known volume (10.77 cm^3) and a manometer (Baratron, MKS). The QMS sensitivities for SEM=1000 and 1200 V were measured to be 3.8×10^{-4} and 7.1×10^{-3} [A/ cm^3 STP], respectively. The detection limit for ^{36}Ar and ^{40}Ar was controlled by the level of residual gases with the same mass numbers (i.e., 36 and 40) and measured to be 1×10^{-11} and 3×10^{-10} [cm^3 STP], respectively.

Age measurement: After calibrating the instruments, we have measured two samples with known K_2O concentration and age: DINO-4 (Hornblende, $K_2O=0.93$ wt%, 1.74 Gyr) and DINO-3 (Biotite, $K_2O=7$ wt%, 1.80 Gyr) [9]. We pressed the pure mineral grains with a cubic press at 4.5 GPa into pellet samples appropriate for LIBS measurements. In order to remove the air adsorbed on the sample surface, the chamber was baked at 180 °C for 24 hours under the vacuum condition. 500 and 1000 laser pulses are irradiated to the hornblende and biotite sample, respectively. Figure 3 shows the LIBS spectrum for the hornblende pellet. Hydrocarbons are removed with the Ti-Zr getter from the gas extracted by laser ablation was

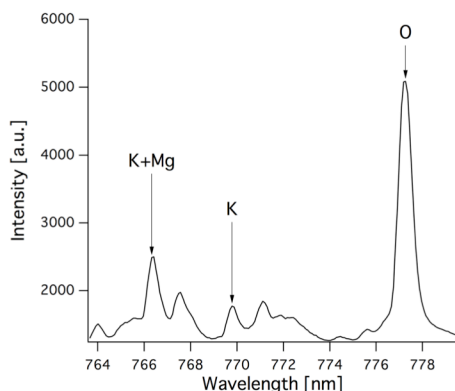


Fig. 3: LIBS spectrum acquired for the hornblende target.

purified and trapped on the cooled charcoal trap while the other part of the vacuum line was evacuated. Finally, the purified Ar gas was released from the trap by raising temperature and was introduced to the QMS for mass spectrometry. Figure 4 shows an example of the mass spectrum obtained in this study. A blank spectrum acquired after the same experimental procedure was subtracted from the mass spectrum. The entire measurement process took approximately 60 minutes.

Using the above calibration curve, we obtained $K_2O=1.0\pm 0.2$ wt% from our LIBS spectrum for DINO-4. This value is consistent with the known concentration of 0.93 wt%. The volume of the crater excavated by laser ablation was measured to be $(4.4\pm 0.5)\times 10^{-5}$ cm³ with a microscopic observation (VHX-2000, Keyence Inc.). Assuming the density of the hornblende sample to be 3.2 ± 0.3 g/cm³, the evaporated mass is estimated to be $(1.4\pm 0.2)\times 10^{-4}$ g, containing $(3.0\pm 0.6)\times 10^{-8}$ mol of K atoms. Assuming $^{40}K/K=^{40}K/(^{39}K+^{40}K+^{41}K)=1.17\times 10^{-4}$ [4], the laser-released ^{40}K was estimated to be $(3.5\pm 0.7)\times 10^{-12}$ mol.

The amount of radiogenic ^{40}Ar extracted from the sample was estimated to be $(2.9\pm 0.6)\times 10^{-8}$ [cm³ STP]= $1.3\pm 0.3\times 10^{-12}$ [mol]. Here, the contribution of atmospheric ^{40}Ar was subtracted from the measured ^{40}Ar based on ^{36}Ar measurement:

$$[^{40}Ar]_{rad}=[^{40}Ar]_{total}-[^{40}Ar]_{atm}=[^{40}Ar]_{total}-296[^{36}Ar],$$

assuming the Ar isotopic ratio in the terrestrial atmosphere ($^{40}Ar/^{36}Ar=296$). Here, $[^{40}Ar]_{total}$, $[^{40}Ar]_{rad}$, $[^{40}Ar]_{atm}$, and $[^{36}Ar]$ refer to the amounts of total ^{40}Ar , radiogenic ^{40}Ar , atmospheric ^{40}Ar and ^{36}Ar in the sample, respectively.

Because the standard sample used in these experiments are highly homogeneous, we cannot obtain an isochron. Thus, we calculate a model age using the following expression:

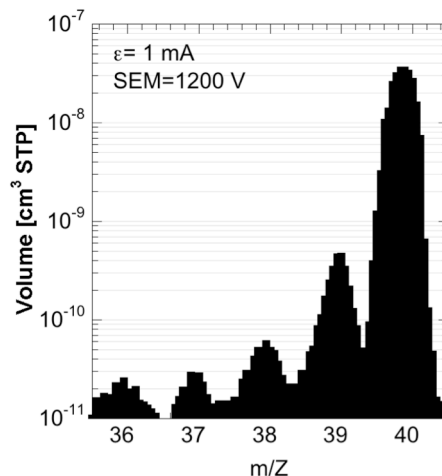


Fig. 4: QMS mass spectrum acquired for the hornblende target.

$$t = \frac{1}{\lambda} \ln \left(\frac{\lambda}{\lambda_e} \frac{[^{40}Ar]_{rad}}{[^{40}K]} + 1 \right),$$

where $\lambda=5.543\times 10^{-10}$ yr⁻¹ and $\lambda_e=0.581\times 10^{-10}$ yr⁻¹ are the total decay constant of ^{40}K and the decay constant of ^{40}K to ^{40}Ar , respectively. $[^{40}Ar]_{rad}$ and $[^{40}K]$ refer to the molar amount of radiogenic ^{40}Ar and the present ^{40}K , respectively. Substitution of the parameters described above yields $t=2.7\pm 0.5$ Gyr. Following the same procedure, the biotite sample yields $K_2O=6.1\pm 0.6$ wt%, crater volume= $(1.3\pm 0.1)\times 10^{-4}$ [cm³], $[^{40}Ar]_{rad}=(4.3\pm 0.7)\times 10^{-11}$ [mol] and $[^{40}K]=(6.1\pm 0.9)\times 10^{-11}$ [mol], resulting in the age of 3.7 ± 0.4 Gyr.

Both of these ages values are larger than the known values by 50%-110%. In other words, 2 - 3 times as much ^{40}Ar as expected was released from the samples. Our preliminary analyses suggest that the additional ^{40}Ar was released from the crater walls via diffusion due to indirect heating by the laser irradiation. A simple geometric estimate shows that heating the crater wall region with thickness 100-200 μm above the closure temperature (~300 °C for hornblende and biotite) would release such excess amount of Ar.

Implications for in-situ age measurements on Mars: Measurement conditions are greatly different depending on the mission target planet. We assess whether we can obtain significant K-Ar ages for typical Mars samples. When we assume 100 μg sample is evaporated by laser shots (corresponding to 500-1000 pulses), radiogenic ^{40}Ar higher than the detection limit (3×10^{-10} cm³) is released from a sample with age of 1 Gyr and K_2O concentration of 1000 ppm. If a sample has 1 wt% K_2O , ~100 Myr rock produces measurable amount of radiogenic ^{40}Ar (Fig. 5). Furthermore, the detection limit of K_2O by LIBS measurement is below 100 ppm. Thus, the LIBS-QMS system can measure

such Martian rocks as the Mars Exploration Rover Spirit found at Gusev crater [10].

Future work: The above results suggest that accurate assessment and reduction of the effect of wall heating and resulting release via diffusion may be very important. Further tuning of laser irradiation conditions, such as pulse repetition rates, may lead to reduction in such Ar release due to diffusion from the laser crater wall.

References:

[1] Doran P. T. et al. (2004) *Earth Sci. Rev.*, 67, 313–337. [2] Cho Y., et al. (2011) *2011 PERC Planetary Geology Field Symposium*, 30. [3] Cho, Y. et al. (2011) *2011 Japan-Korea joint meeting of Isotope-ratio Mass Spectrometry*, Abstract #3. [4] Steiger R. H. and Jäger E. (1977) *EPSL*, 36, 359-362. [5] Talboys D. L. et al. (2009) *PSS*, 57, 1237-1245. [6] Swindle T. et al. (2003) *LPS XXXIV*, Abstract #1488. [7] Harris R. D. et al. (2005) *LPS XXXVI*, Abstract #1796. [8] Stipe C. B. et al. (2012) *Spectrochim. Acta B*, 70, 45–50. [9] Nagao K. (2012) personal comm. [10] Ming D. W. et al. (2008) *JGR*, 113, E12S39.

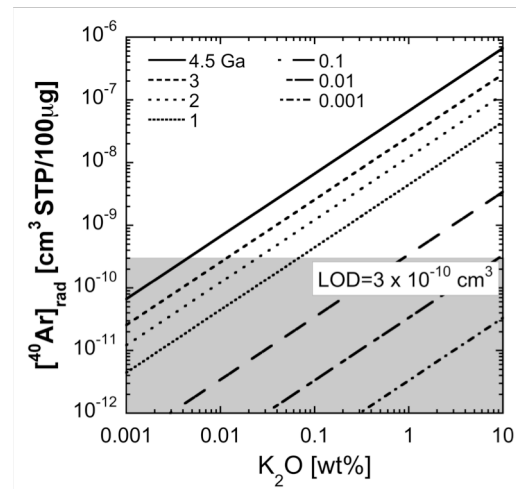


Fig. 5: The amount of ^{40}Ar produced from a sample with different K_2O concentration and age. Samples with K_2O and age in the white area yield the detectable amount of ^{40}Ar .